EurAsian Journal of BioSciences
Eurasia J Biosci 14, 2969-2974 (2020)

Synthesis and study electrical properties of new polymer Copper Oxide NanoComposite

Azhar Farooq [1*], Maida H. Saleem [1], Basma J. Ahmed [1]

[1] Department of Chemistry, College of Education for Pure Science /Ibn-Al-Haitham, University of Baghdad, IRAQ
*Corresponding author: azhaar.442006@gmail.com

Abstract

Cupric oxide nanoparticles CuO NPs can be produced by sol-gel. The copper oxide nanocomposite (CuO/PAG) was prepared by added suspension solution of CuO NPs to polymer blend (PAG) which was prepared by mixing poly acetal resin with gelatin. The nanoparticles morphology is categorized through powder X-ray diffraction (XRD) along with scanning electron microscopy (SEM). Using the Scherrer formula, the average crystallite size of CuO nanoparticles can be computed. The analysis of powder XRD shows a formed monoclinic CuO phase with 15 nm average particle size. There is good agreement between the data obtained by XRD and microscopic measurements. The electrochemical characteristics for synthesized nanocomposite have been examined. The dielectric performance for a sample involving dielectric loss, AC conductivity and dielectric constant has been recorded under numerous frequency levels.

Keywords: Copper Oxide, Conductivity, NanoComposite, Resin

Farooq A, Saleem MH, Ahmed BJ (2020) Synthesis and study electrical properties of new polymer Copper Oxide NanoComposite. Eurasia J Biosci 14: 2969-2974.

INTRODUCTION

Generally, numerous metal oxides are obtainable in the nature, but several metal oxides have been in higher practicality based on their regular applications in their scientific and technological fields. The transition metals in the periodic table have been copious based on copious application fields. Several transition metal oxides examples are ZnO, TiO2 and Fe3O4, etc. They turned out to be potential candidates for so many applications. Similarly, CuO has been as well one of an advantageous metal oxides with countless applicable fields. The distinctiveness for CuO nanoparticles is that, while they have been metallic plentifully, they act similar to semiconductors in term of nanometric size. Semiconductor materials are predominantly remarkable due to their huge applied significance in optoelectronic and electronic devices like electrochemical cells (Rai et al. 2019) gas sensors (Katti et al. 2003) , magnetic recording devices (Liu et al. 2012; Olayiwola, et al, 2015), field emitters (Hsieh et al. 2003), superconductors high tc (Sagadevan et al. 2018) , nano fluid (Chang et al. 2011) and catalysts (Zhang et al. 2019) , etc. As a result of potential CuO, it behaves as a catalyst. Nonetheless, all metal oxides have been not advantageous for catalytic actions. The manufacture of super capacitors with CuO has been highly practical. It has a broadband gap almost equivalent to ZnO within nano range. A favorable band separation of CuO of about 2.6 eV creates it suitable for the solar energy conversion, and it is feasibly employed as a solar cell window material. Nano-fluids stands for applicable refrigerant in refrigerators. These nanofluids are integrated with the carrier liquid for improving energy transfer as compared to the carrier liquid lonely. CuO is feasibly employed as a refrigerant material, and it effectively acts as temperature controller as similar as other TiO2 refrigerants, silver and alumina particles, etc. The nanomaterials characteristics rely mainly on the nanopowders size, the morphology and the particular surface area of the primed materials. Several features depend very much on the preparation approaches. Previous studies on CuO nanocrystals had given different physical, chemical and electrical binding features. Lattice tension and structural disorder feasibly varies the material properties in diverse applicable fields of chemical engineering. There are several approaches for manufacturing CuO nanoparticles. Among those who have chosen the sol-gel method for the preparation of CuO nanoparticles. One of them has been in higher preference and extensively adopted in synthesizing the nano particles. The particle size of the various preparing methods are listed. For MOCVD [metal-organic chemical vapor deposition], the size of CuO nanoparticles is ranged from 0.05 to 8 μm (Condorelli et al. 1999). The sonochemical method has been around

Received: February 2019
Accepted: March 2020
Printed: September 2020

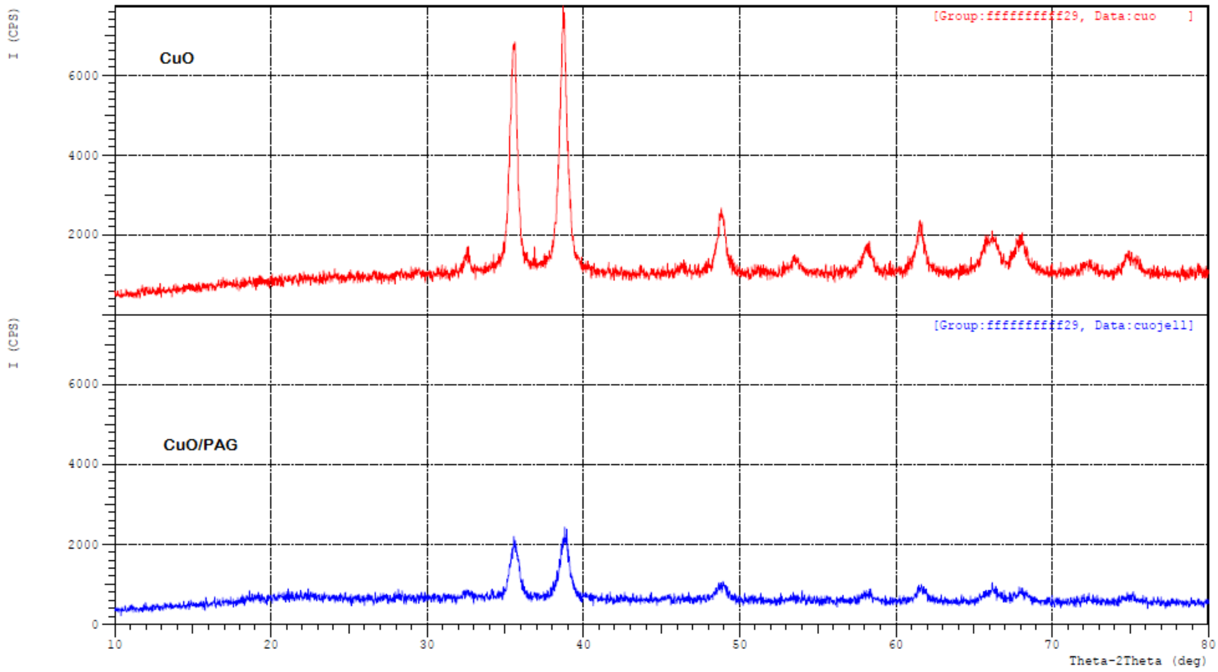

Fig. 1. XRD Patterns of CuO NPs and CuO/PAG

10 nm to some microns (Vijaya et al. 2001). Several consequences have shown in several reported papers within CuO nanoparticles range of 18-20 nm in the sol-gel method (Aparna et al. 2012). An average diameter for CuO nanoparticle in solid state reaction is reported in the range of 15-20 nm (Cao et al. 2004). Smaller CuO nanoparticles have practiced by electrochemical process with a size of about 4 nm (Borgohain et al. 2000).

MATERIAL AND METHODS

Preparing CuO Nanoparticles

CuO nanoparticles have prepared through sol-gel method. An aqueous solution of $CuNO_3.6H2O$ (0.1 M) was put in round bottom flask, then was heated to 65ºC with continuous stirring. About 0.5 M NaOH has inserted to above heated solution until pH is reached to 12. The solution color is changed to dark blue green instantaneously. The precipitate was centrifuged and washed three to four times with deionized water. The gotten precipitate turned to black after drying it in oven for complete day at 100ºC. This CuO powder was employed for the material characterizing (Aparna et al. 2012, p. 157).

Synthesis of Resin

The resin was prepared from dissolved (1.38)g of Pentaerythritol [$C_5H_{12}O_4$]with (0.31) g Glutaraldehyde [$C_5H_8O_2$] in the presence of a catalyst drying agent [$ZnCL_2$] in (15ml of benzene, 4ml of ethanol and two drops of HCL acid) and heat under reflux at 70°C for 72 h. The polyacetal formed has precipitated in the mixture of cold solvent of Et_3N: MeOH (2: 5). Subsequently, the precipitate has filtered, bathed and dried at 50 ° C overnight under vacuum (Cohen et al. 1962).

Synthesis of Film Blended (PAG)

Poly acetal resin was blended with gelatin (1:1) to prepare thin film (PAG). Solution of resin was prepared by dissolved (0.5)g in 100ml distillated water. After that, 0.5 g of gelatin was added with mixture by mechanical stirrer for 1h at room temperature and poured into the mold of (5x5)cm^2.

Synthesis of Copper Oxide Nanocomposite (CuO/PAG)

Suspension solution of CuO NPs was dispersion by ultrasonic. The same method used as prepared PAG except added suspension of CuO NPs (1%).

The crystalline phases of CuO nanoparticles and its composite have investigated based on X-ray Diffractorometer (XRD) using CuKα as radiation source (40 kV, step size 0.020, scan rate 0.50 min^{-1}). The morphology of the prepared samples was carried out through scanning electron microscope (SEM, Hitachip-SEM S- 3400n, Germany).

RESULTS

XRD Analysis

The XRD analysis has given sequential diffraction peaks at 2θ of 32.56, 35.54, 38.73, 48.81, 53.52, 58.15, 61.53, 66.22, 67.92, 72.23, and 74.77 which can be consigned to (110), (–111), (111), (–202), (020), (202), (–113), (–311), (220), (311), and (004) planes, respectively (**Fig. 1**). All diffraction peaks well matched the monoclinic CuO phase (standard JCPDS File No. 45-0937). The average crystallite size of CuO NPs has

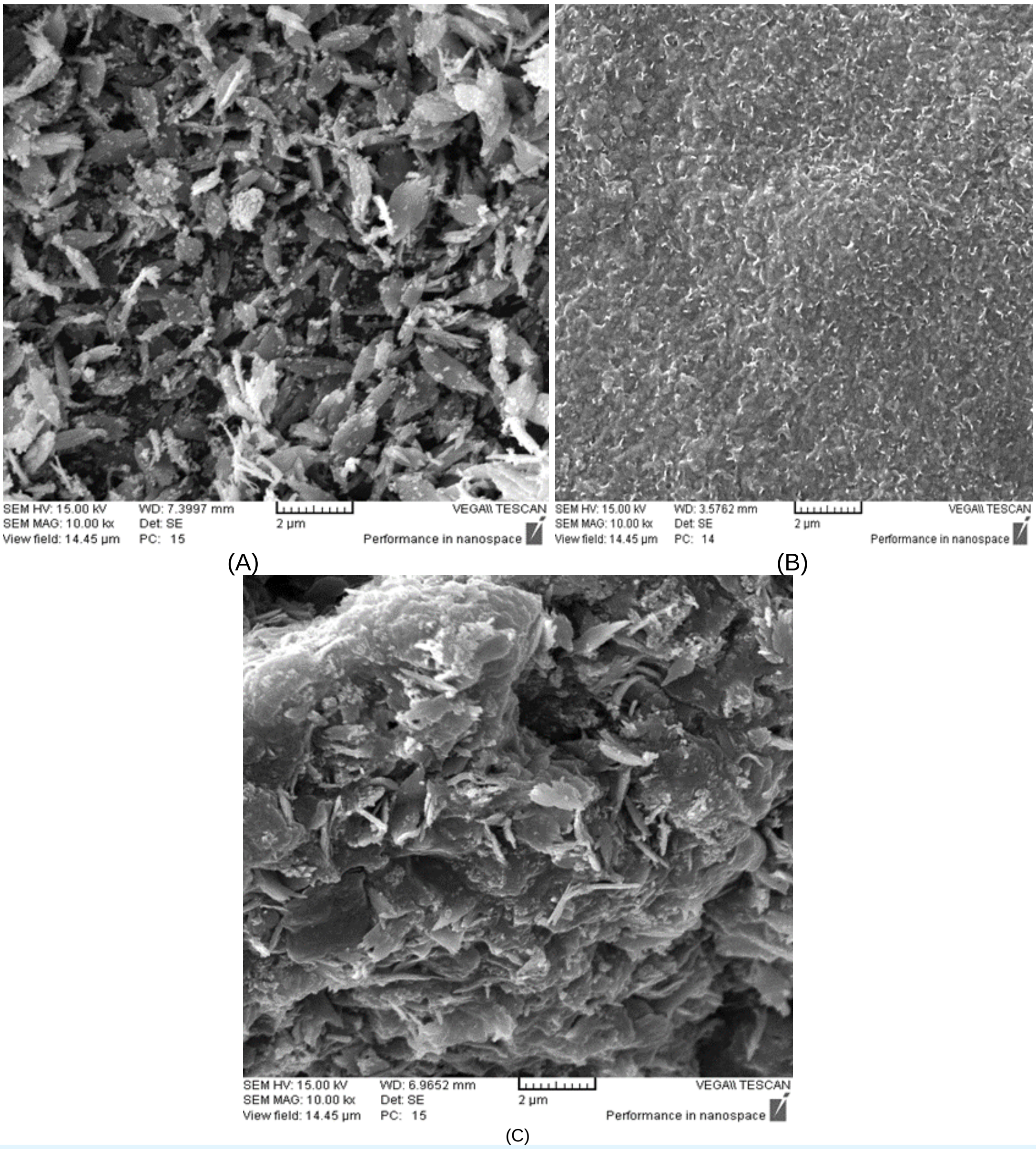

Fig. 2. SEM Images of a: CuO NPs, b: PAG, and C: CuO/PAG

computed using the Scherrer formula: D = 0.9λ/βcosθ, where D stands for a crystallite size (nm); β represents a full width at half maximum of the peak; λ has been the X-ray wavelength of CuKα = 1.54 A, and θ is the Bragg angle (Klug and Alexander 1974) . The same peak was appeared in XRD pattern for CuO/PAG but with law intensity which indicated the existence of an amorphous structure (Aleksandrov et al. 2015). An average grain size computed through Debye-Scherrer formula is about 15 nm.

SEM Analysis

The SEM images of CuO have been explained by **Fig. 2a**. The recorded SEM images in 2 µm magnification have shown a distinct and interesting particles shapes with seamless arrangement. The CuO nanoparticles have been as jasmine buds. During looking at close up, it was given many details concerning the rearrangement and structure. The buds like particles have been satisfactorily disconnected from each other. **Fig. 2b** gives clear depiction about surface morphology of PAG while 2C image for CuO/PAG surface at similar magnification, shows a modification of surface texture for PAG.

Study of Electrical Properties

Conductivity investigations and dielectric behavior in **Fig. 3**, explain the behaviour of dielectric constant έ with frequency for CuO, PAG and CuO/PAG at room temperature. Accordingly, it is perceptible that the real amount of dielectric constant always drops swiftly as frequency increases. As frequency increases, έ reaches constant value. CuO explains the highest magnitude of dielectric constant than CuO/PAG. However, PAG was

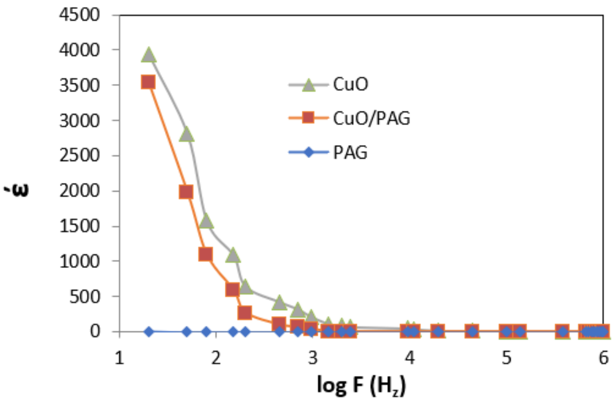

Fig. 3. Dielectric Constant (έ) vs log Frequency for CuO, CuO/PAG, PAG

in a performance of the insulating material with raised frequency. The electron interchange between a polymer chain and CuO provides a limited electrons shift that generates polarization in a blend nanocomposite. Nanostructured CuO stands for the carrier dominated dielectric and gives frequency dispersion as a result of space charge polarization. The interfaces with huge fractions in dielectric nanostructured samples have many defects including vacancies, dangling bonds, micro porosities and vacancy clusters that result in changed positive and negative space charge distribution in interfaces (Kumar and Ravinder 2002). In the case of it is subjected to the electric field, these space charge will be moved. As they have been trapped by defects, numerous dipole moments can be established. In low frequencies, these dipole moments are straightforwardly go along with the electric field change. Henceforth, the dielectric constant has been huge at low frequency. In typical dielectric performance, the dielectric constant stays practically constant at high frequency. This is due to intrawell hopping becomes prominent and the charge carriers don't have sufficient time for extensive range hopping before field reversal beyond certain frequency for the electric field. Consequently, only intrawell hopping occurs in the high-frequency region owing to an average hopping distance for intrawell hopping with single lattice space. intrawell hopping has been within a few nanometers. In consequence, polarization lessens as the signal frequency has been raised (Patil et al. 2000).Dielectric loss (ε̋) as a frequency function ranged from 20 –10^6 Hz under room temperature for the CuO,CuO/PAG, and PAG are plotted in **Fig. 4**. It is revealed that the dielectric loss as well lessens precipitously as frequency raises (Yang et al. 2020).A.C. electrical Conductivity (σ) in **Fig. 5**, describes the AC conductivity of CuO, CuO/PAG and PAG at dissimilar frequencies. It has been obvious from **Fig. 5** that AC conductivity of CuO has considerably greater as compared with the CuO/PAG. The conductivity has been raised with frequency. The composite conductivity is subjected to macroscopic and microscopic

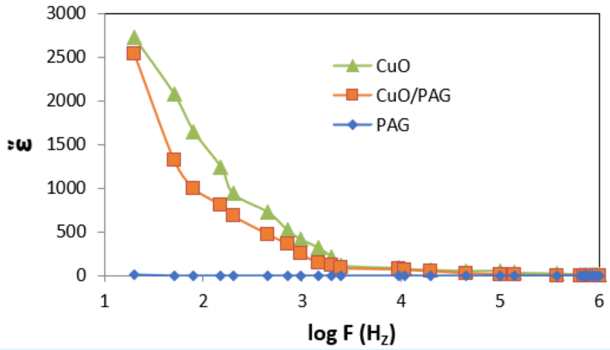

Fig. 4. Dielectric Loss (ε̋) vs log Frequency for CuO, CuO/PAG, PAG

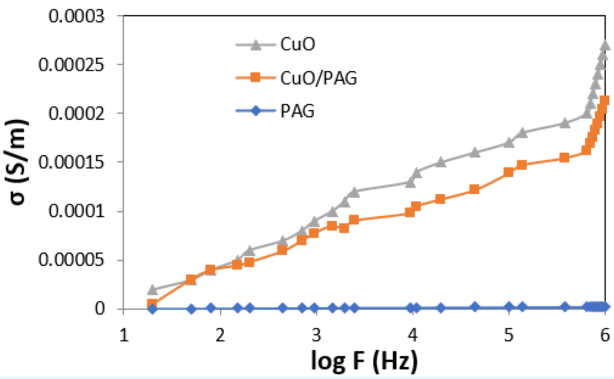

Fig. 5. AC Conductivity (σ) vs log Frequency for CuO, CuO/PAG, PAG

conductivities. The microscopic conductivity is subjected to an interacted molecules, chain length and conjugation length. The macroscopic conductivity is subjected to homogeneities in the composites, pellets compactness, microparticles orientation, etc. In the current research article, a nanocrystalline behavior of CuO particles is possibly given rise to upsurge in composites orderliness that is set by XRD and SEM. This orderliness raises the smallness and molecular orientations with increased macroscopic conductivity (Ramesan 2012).

CONCLUSIONS

An uncomplicated and economical strategy was developed in this study for obtaining CuO/PAG nanocomposites. Homogenous dispersion of CuO with monoclinic phase has detected over the PAG surface. Surface morphological properties based on shape and particle size have demonstrated through SEM analysis. The PAG electrochemical performance has been boosted as a result of copper oxide nanoparticles in its matrix. Therefore, the electrochemical fallouts put forward that CuO/PAG nanocomposite has been a noticeable choice for efficient supercapacitor devices. The dielectric loss, dielectric constant and AC conductivity have investigated, and the magnitudes have estimated at diverse frequencies and room temperature. The dielectric constant and dielectric loss magnitudes have been inversely proportional with the increased frequency.

ACKNOWLEDGEMENTS

The authors would like to give thanks and appreciation to all members of the Central Service Laboratory in the College of Education for Pure Sciences/ Ibn Al-Haitham, for providing assistance in carrying out this research.

REFERENCES

Aleksandrov, V. A., Ostaeva, G. Y., Papisova, A. I., Papisov, I. M., Prikhod'ko, V. M., & Fatyukhin, D. S. (2015, August). Synthesis of a copper–polymer nanocomposite on the steel surface. In Doklady Chemistry, 463(2): 204-207. Pleiades Publishing. https://doi.org/10.1134/S0012500815080029

Aparna, Y., Rao, K. E., & Subbarao, P. S. (2012). Synthesis and characterization of CuO nano particles by novel sol-gel method. In Proceedings of the 2nd International Conference on Environment Science and Biotechnology. DOI: 10.7763/IPCBEE. 2012. V48. 30

Borgohain, K., Singh, J. B., Rao, M. R., Shripathi, T., & Mahamuni, S. (2000). Quantum size effects in CuO nanoparticles. Physical Review B, 61(16): 11093. https://doi.org/10.1103/PhysRevB.61.11093

Cao, Y. L., Jia, D. Z., Liu, L., & Luo, J. M. (2004). Rapid synthesis of lead oxide nanorods by one-step solid-state chemical reaction at room temperature. Chinese Journal of Chemistry, 22(11): 1288-1290. https://doi.org/10.1002/cjoc.20040221115

Chang, M. H., Liu, H. S., & Tai, C. Y. (2011). Preparation of copper oxide nanoparticles and its application in nanofluid. Powder technology, 207(1-3): 378-386. https://doi.org/10.1016/j.powtec.2010.11.022

Cohen, S. M., Hunt, C. F., Kass, R. E., & Markhart, A. H. (1962). Polyspiroacetal resins. Part II. Structure and properties of polyspiroacetals from pentaerythritol-glutaraldehyde and from (pentaerythritol–dipentaerythritol)-glutaraldehyde. Journal of Applied Polymer Science, 6(23): 508-517. https://doi.org/10.1002/app.1962.070062304

Condorelli, G. G., Malandrino, G., & Fragalà, I. L. (1999). Nucleation and Growth of Copper Oxide Films in MOCVD Processes Using the β-Ketoiminate Precursor 4, 4′-(1, 2-Ethanediyldinitrilo) bis (2-pentanonate) Copper (II). Chemical Vapor Deposition, 5(5): 237-244. https://doi.org/10.1002/(SICI)1521-3862(199910)5:5<237::AID-CVDE237>3.0.CO;2-U

Hsieh, C. T., Chen, J. M., Lin, H. H., & Shih, H. C. (2003). Field emission from various CuO nanostructures. Applied Physics Letters, 83(16): 3383-3385. https://doi.org/10.1063/1.1619229

Katti, V. R., Debnath, A. K., Muthe, K. P., Kaur, M., Dua, A. K., Gadkari, S. C., ... & Sahni, V. C. (2003). Mechanism of drifts in H2S sensing properties of SnO2: CuO composite thin film sensors prepared by thermal evaporation. Sensors and Actuators B: Chemical, 96(1-2): 245-252. https://doi.org/10.1016/S0925-4005(03)00532-X

Klug, H. P., & Alexander, L. E. (1974). X-ray diffraction procedures: for polycrystalline and amorphous materials, Wiley, united state.: 992. https://ui.adsabs.harvard.edu/abs/1974xdpf.book.....K/abstract

Kumar, B. R., & Ravinder, D. (2002). Dielectric properties of Mn–Zn–Gd ferrites. Materials Letters, 53(6): 437-440. https://doi.org/10.1016/S0167-577X(01)00522-5

Liu, L., Xiao, L., Zhu, H., & Shi, X. (2012). Preparation of magnetic and fluorescent bifunctional chitosan nanoparticles for optical determination of copper ion. Microchimica acta, 178(3-4): 413-419. https://doi.org/10.1007/s00604-012-0855-9

Olayiwola, M. O., Soremi, P. A. S., & Okeleye, K. A. (2015). Evaluation of some cowpea [Vigna unguiculata (L.) Walp.] genotypes for stability of performance over 4 years. Current Research in Agricultural Sciences, 2(1), 22-30.

Patil, A. N., Patil, M. G., Patankar, K. K., Mathe, V. L., Mahajan, R. P., & Patil, S. A. (2000). Dielectric behaviour and ac conductivity in $Cu_xFe_{3-x}O_4$ ferrite. Bulletin of Materials Science, 23(5): 447-452. https://doi.org/10.1007/BF02708397

Rai, S., Bhujel, R., Biswas, J., & Swain, B. P. (2019). Effect of electrolyte on the supercapacitive behaviour of copper oxide/reduced graphene oxide nanocomposite. Ceramics International, 45(11): 14136-14145. https://doi.org/10.1016/j.ceramint.2019.04.114

Ramesan, M. T. (2012). In situ synthesis, characterization and conductivity of copper sulphide/polypyrrole/polyvinyl alcohol blend nanocomposite. Polymer-Plastics Technology and Engineering, 51(12): 1223-1229. https://doi.org/10.1080/03602559.2012.696766

Sagadevan, S., Zaman Chowdhury, Z., Johan, M. R. B., Aziz, F. A., Salleh, E. M., Hawa, A., & Rafique, R. F. (2018). A one-step facile route synthesis of copper oxide/reduced graphene oxide nanocomposite for supercapacitor applications. Journal of Experimental Nanoscience, 13(1): 284-296. https://doi.org/10.1080/17458080.2018.1542512

Vijaya Kumar, R., Elgamiel, R., Diamant, Y., Gedanken, A., & Norwig, J. (2001). Sonochemical preparation and characterization of nanocrystalline copper oxide embedded in poly (vinyl alcohol) and its effect on crystal growth of copper oxide. Langmuir, 17(5): 1406-1410. https://doi.org/10.1021/la001331s

Yang, X., Fan, S., Li, Y., Guo, Y., Li, Y., Ruan, K., ... & Gu, J. (2020). Synchronously improved electromagnetic interference shielding and thermal conductivity for epoxy nanocomposites by constructing 3D copper nanowires/thermally annealed graphene aerogel framework. Composites Part A: Applied Science and Manufacturing, 128, 105670. https://doi.org/10.1016/j.compositesa.2019.105670

Zhang, K., Suh, J. M., Lee, T. H., Cha, J. H., Choi, J. W., Jang, H. W., ... & Shokouhimehr, M. (2019). Copper oxide–graphene oxide nanocomposite: efficient catalyst for hydrogenation of nitroaromatics in water. Nano convergence, 6(1): 6. https://doi.org/10.1186/s40580-019-0176-3